Layered materials with high strength and flaw tolerance based on alumina and aluminium titanate

Salvador Bueno, Carmen Baudín

Instituto de Cerámica y Vidrio, CSIC

Campus de Cantoblanco, 28049 Madrid, Spain

Abstract. Laminates in which high strength external layers and flaw tolerant internal layers with similar compositions are combined, can provide improved mechanical behavior in relation to that of monolithic materials with the same composition as the layers. The limitation of this design, in which no residual stresses are present, is the difficulty that involves the co-sintering of layers with large microstructural differences in the green state. This work describes a new method to obtain laminates constituted by layers with large differences in terms of grain size starting from green bodies with similar microstructures. The approach is based on the effect of small amounts of titania as agents for alumina grain growth enhancement. Starting from fine grained green bodies that combined alumina layers with composite layers made of mixtures of alumina and titania, additional "in situ" formed layers constituted by large (≅20-30μm) alumina grains were found after sintering contiguous to the composite layers. The thickness of the "in situ" formed layers reached up to 200 μm, depending on the thermal treatment (1450-1550ºC). The fracture behaviour of the laminates and the monoliths was studied, using stable SEVNB (Single Edge V Notched Beam) tests, in terms of work of fracture and the critical stress intensity factor in mode I, K_{IC}. The large grain sized alumina layers reinforced the laminates by crack branching and bridging.

Keywords: laminates; Al_2O_3; Al_2TiO_5; grain size; toughness and toughening

1. Introduction

Alumina materials are widely used in applications where hardness, wear and/or chemical resistance are required but traditionally the applications as structural components have been limited due to the lack of reliability associated to the brittle fracture mode. Structures found in nature such as biological hard tissues, shells and teeth are made of layered architectures combining materials with different properties that lead to laminates with mechanical behaviour superior than that of the individual constituents[1-3]. In this sense, much research is being devoted to the development of laminates to improve the performance of brittle materials. Laminates emerge as a new strategy to achieve "flaw tolerance" in opposition to the traditional "flaw elimination" approach of monolithic ceramics.

In particular, laminated structures where alternating high-strength external layers and internal flaw tolerant layers are combined might provide fracture resistance keeping the high strength of the surface layers. This approach has been proposed as a way to overcome the low strength values of the flaw tolerant alumina (Al_2O_3)-aluminium titanate (Al_2TiO_5) composites[4-7]. Major limitation is the presence of tensile residual stresses in the external layers since the high strength compositions in this system usually present larger thermal expansions and Young's modulus than the flaw tolerant ones[5-6]. The combination of homogeneous external layers with highly heterogeneous layers with similar composition has been proposed as means to avoid the development of significant residual stresses[4]. The limit of this approach is the difficulty that involves the co-sintering of layers with such microstructural differences. One solution is the fabrication of graded materials in which transitional microstructures are tailored

between both surfaces of the samples through a green processing in several steps, as it allows reaching specific surface properties different than those of the bulk[8-9].

In this work, a way to obtain laminates with large microstructural differences between contiguous layers, based on the effect of small amounts of titania (TiO_2) as agent for alumina grain growth enhancement[10-11], is analysed. The designed structure is constituted of high strength external layers of small grain sized alumina combined with flaw tolerant internal layers[12-13] (Fig. 1). In the green state, alumina layers are combined with composite layers made of mixtures of alumina and titania. The effect of titania leads to interlayers of large grain sized alumina to be formed between the alumina and the composite layers (Fig. 1). As the microstructural heterogeneity is developed during sintering, no decohesion of the layers due to differential sintering occurs. Although titania diffusion might take place during the whole thermal cycle, it would be more extensive at high temperatures once initial co-sintering of the layers has taken place so, the thickness of the large grain sized alumina layer formed “in situ” could be controlled through the adequate selection of the thermal treatment.

In order to evaluate quantitatively the effect of the "in situ" formed layers, toughness and work of fracture of the laminates and of monoliths of the same compositions as those of the initial layers have been compared. The work of fracture, γ_{WOF}, is defined by the mean external work which is consumed to produce a unit of fracture surface area during quasi-static failure and is determined experimentally from the total area under the load-load point displacement curve in stable tests. This parameter provides significant toughness values because no spare energy is involved in the test and, therefore, the whole energy given to the system is employed in creating new surfaces. Nevertheless, the difficulty to get stable tests in brittle materials has usually restricted the use of work of fracture to the characterization of the reinforcement in materials with

non-linear behaviour where numerous energy consuming processes can occur during fracture. The energy principle is based on macroscopic thermodynamics and does not require any assumptions regarding the constitutive equation of the cracked body for discussing crack-growth problems[14]. This feature enables the application of the energy principle to characterise nonlinear deformation and fracture behaviours as well as oriented structures such as laminates.

2. Experimental

Monoliths of monophase alumina (A) and alumina+10vol.% aluminium titanate (A10AT), and one layered structure combining two external and one central alumina layers with two internal alumina+10vol.% aluminium titanate composite layers (Fig. 1) were manufactured by a colloidal route from aqueous Al_2O_3 and TiO_2 suspensions using the optimum green processing conditions previously established[5,15]. The starting materials were commercial α-Al_2O_3 (Condea, HPA05, USA) and TiO_2-anatase (Merck, 808, Germany) powders. The single oxide (Al_2O_3) and the mixture (Al_2O_3/TiO_2) were dispersed in deionised water by adding 0.5wt.% (on a dry solids basis) of a carbonic acid based polyelectrolyte (Dolapix CE64, Zschimmer-Schwarz, Germany). Suspensions were prepared to a solids loading of 50 vol.% and ball milled with Al_2O_3 jar and balls during 4h.

Plates of monolithic and laminated materials with 70x70x10 mm^3 dimensions were obtained by slip casting, removed from the moulds and dried in air at room temperature for at least 24h. The layered plates, constituted by five layers, with thick external and central layers of alumina (1300μm) and two thin intermediate layers of the composite (300μm), were fabricated by alternately casting the suspensions. Casting times were fixed to reach the desired layer thickness considering the casting kinetics and sintering

shrinkage of each composition[5]. The dried blocks were sintered in air in an electrical box furnace (Termiber, Spain) at heating and cooling rates of 2ºCmin^{-1}, with 4h dwell at 1200ºC during heating and two different treatments at the maximum temperature: 2h dwell at 1450ºC and 3h dwell at 1550ºC. For all tests, samples were diamond machined from the sintered blocks.

Microstructural characterization was performed by field emission scanning electron microscopy (FE-SEM, Hitachi, S-4700, Japan) on polished and thermally etched (20ºC below the sintering temperature during 1 min) or chemically etched (HF 10vol% - 1min) surfaces. The average grain size was determined by the linear intercept method considering at least 200 grains for each phase.

The profiles of titania in the laminates were determined by wavelength dispersive X-ray spectrometer, WDS, (JEOL, Superprobe JXA-8900 M, Japan) on polished cross surfaces of the laminate, operating at 15 kV, 20nA and 10s in the peak position. The k-factors in the quantification were calculated using the atomic number-absorption-fluorescence (ZAF) correction. The analysis was made along three straight lines perpendicular to the layers, taking spots with 5μm diameter, and the average of the three determinations was associated to each corresponding localization across the polished surface the specimen.

Single-Edge-V-Notch-Beams (SEVNB) of 4x6x50mm^3 of the monoliths and the laminates were tested in a three point bending device using a span of 40mm and cross head speed of 0.005mm·min^{-1} (Microtest, Spain). The notches were initially cut with a 150 μm wide diamond wheel to a depth of about 70% of the final depth. Using this slot as a guide, the remaining part of the notch was done with a razor blade sprinkled successively with diamond paste of 6 and 1μm. The depth of the notches, a, was approximately 0.5 of the thickness of the monolithic samples (W) and 0.14 and 0.28 of

the thickness of the laminated samples, which resulted in a relation $a/W_A \cong 0.4$ and 0.8 respectively for the width of the external alumina layer, W_A, in the laminated samples (Fig. 1). The tip radii of the notches were optically observed to check that they were below 30μm. The curves load versus displacement of the loading frame were recorded during three tests for each material. Fracture toughness, K_{IC}, values were calculated according to a general stress intensity formulation valid for any crack length[16] and the work of fracture, γ_{WOF}, values were obtained by dividing the area under the stable load-displacement curves by twice the area of the un-notched part of the cross section of the samples. FE-SEM was performed on the fracture surfaces.

The crack path in the notched samples was characterized by optical microscopy (H-P1, Zeiss, Germany) of the polished lateral faces.

3.- Results

Characteristic microstructures of the monolithic materials are shown in Fig. 2 and the microstructural parameters are summarised in Table 1 together with the values of fracture toughness and work of fracture. The alumina materials (Fig. 2a, 2c) presented different levels of grain growth (Table 1), being the microstructure of the alumina sintered at the highest temperature (1550ºC, Fig. 2c) bimodal with some grains larger than 10μm and the rest of the grains in the range described by the average size determined by the linear intercept method (Table 1). In the composites, aluminium titanate was homogeneously distributed and mainly located at alumina triple points and grain boundaries, and no titania was observed by this method (FE-SEM).

There were not significant differences in the values of fracture toughness (Table 1) for the alumina materials, whereas the work of fracture values were higher for the specimens sintered at 1550ºC. In the composites, considerably higher values of work of

fracture were achieved in relation to monophase aluminas and an increase with the sintering temperature was also observed. The fracture toughness values of the composites were slightly higher than those of alumina and similar for both sintering temperatures.

The microstructures of the obtained laminated structures are shown in Fig. 3. In the samples sintered at 1450ºC the thickness of the "in situ" developed large grain sized alumina layers was less than 80 μm (Fig. 3a) and was formed by grains with sizes up to 20 μm (Fig 3c). In the specimens sintered at 1550ºC the thickness was about 150 μm (Fig. 3b) and the layers had extremely bimodal microstructures, as those reported for TiO_2-doped aluminas[10-11], constituted of groups of small (≅2-3μm) alumina grains surrounded by very large (> 20-30 μm, Fig. 3d) ones. For both laminates, the initial external and central alumina layers as well as the internal composite layers (Fig. 3c and 3d) presented microstructures similar to those of the corresponding monoliths (Fig. 2, Table 1) with similar average grain sizes: 3.2±0.2 μm and 2.9±0.2 μm for alumina grains in the fine alumina and composite layers respectively in the laminate sintered at 1450ºC; and 5.2±0.3 μm and 3.9±0.2 μm in the fine alumina and composite layers respectively in the laminate sintered at 1550ºC.

Figure 3c-d presents the profiles of titania content in the alumina layers. Significant TiO_2 amounts, up to 0.08 and 0.15 mol% in materials sintered at 1450 and 1550ºC respectively, were found at both sides of the composite layers with a decreasing trend through the widths of the contiguous large grained alumina layers.

Characteristic load-displacement curves of notched samples of the laminates are shown in Fig. 4. The tests of specimens with relative notch size of 0.4 of the width of the external alumina layer (Fig.1) were unstable for the materials sintered at 1450ºC and semi-stable for the materials sintered at 1550ºC. For larger notch depths (0.8 of the

width of the external alumina layer, Fig. 1) all tests were semi-stable and, therefore, suitable for the determination of work of fracture.

The fracture toughness and work of fracture values for the laminates are included in Table 2. In the laminate sintered at low temperature, fracture toughness was independent of the notch depth. This trend could not be checked for the work of fracture due to the unstable behaviour of the samples with the shortest notch. Conversely, in the laminate with thicker "in situ" formed large grain sized alumina layer there was a decrease in fracture toughness and work of fracture when the tests were performed with the longest notch depth.

In Figures 5-6, characteristic fracture surfaces of the layered specimens are shown. For both materials, fracture was mixed trans/intergranular in the fine grained alumina layers, being the largest grains the ones most frequently traversed by the crack (Figs. 5a, 6a-b), and was intergranular in the large grained alumina layers (Figs. 5b-c, 6b-c). In these latter, numerous pores located at the grain boundaries were revealed by the fracture. In the specimens sintered at 1550ºC and with the largest notch, fracture started from the large grain sized internal layer (Fig. 6c) whereas in the other specimens, fracture started from the surface fine alumina (Figs. 5, 6 a-b).

Both parts of the specimens remained together after testing (Fig. 7) when stable fracture was attained. The crack path was quite straight in the laminated specimens sintered at low temperature (Fig. 7a) whereas it was extremely tortuous in the materials sintered at 1550ºC. In these latter, large alumina grains of the "in situ" formed coarse layers acting as sites for crack branching and bridges in the wake of the propagating crack were observed (Fig. 7b).

4.- Discussion

Both laminates presented the expected microstructural development (Fig. 3), with "in situ" formed layers of large grain sized alumina at both sides of the composites layers (Fig. 3a and 3b). There was a complete agreement between maximum sintering temperature, thickness of the "in situ" formed large grained alumina layers and extension of titania diffusion, which verifies the suitability of the proposed processing method to obtain large microstructural differences from similar green bodies. The unexpected high levels of porosity observed at the grain boundaries in the large grained alumina layers (Figs. 5c, 6c) have to be related to the effect of TiO_2 during sintering as occurs in TiO_2-doped mullite[17], and their origin has to be further analysed. Nevertheless, what is clear is the strong effect of this intergranular porosity on the fracture characteristics of the considered layers.

In general, the fracture mode of alumina materials has a strong dependence on grain size. Materials with mean grain size in the range 3-20 μm showed both transgranular and intergranular behaviour and the proportion of intergranular fracture decreased rapidly with increasing grain sizes, so the dominant fracture mode was transgranular for mean grain sizes larger than 10-20 μm [18]. In alumina materials with mean grain size of 20 μm and R-curve behaviour, intergranular fracture was also observed for very large grains, in the order of 100 μm, acting as bridges[19]. The fractographic observations in this work, Fig. 5 and Fig. 6, show that effectively the fine alumina layers (Fig. 5a and 6a), with relatively small alumina mean grain size (3.2 and 5.2 μm at 1450 and 1550ºC respectively), presented a mixed inter/transgranular fracture, whereas the "in situ" formed large grained alumina layers presented intergranular fracture, even for grains with sizes in the range of or larger than 20-30 μm (Fig. 6b and 6c). This mode of

fracture is explained by the presence of the extensive intergranular porosity (Fig. 5c, 6b and 6c) that provide grain boundaries weak enough to change the fracture fronts.

These laminated structures developed low residual stresses during cooling from sintering due to the similarity between the thermal expansions of the layers. Approximately constant compressive stresses of about 20 MPa and tensile stresses from about 20 MPa at the interface to 2 MPa at the interior in the alumina and composite layers, respectively, have been determined for the material sintered at 1550ºC[13]. This distribution of residual stresses explains the similarity of the fracture toughness values of the laminates (Table 2) and the monolithic alumina materials obtained at the same conditions (Table 1). In the absence of residual stresses, the mechanical behaviour of ceramic laminates formed by non-interacting layers, such as those fabricated from micron-sized particles of compatible phases, should be derived from the mechanical properties of monoliths with the same compositions as those of the layers and processed in the same way as the laminates.

In order to analyse the work of fracture values of the laminates (Table 2) the combination of alumina with composite layers, with different mechanical response has to be considered. As terms of comparison, the linear combination of the work of fracture values of the monoliths using as relative weight the volume fraction of each composition in the laminate (v_{A10AT}=0.1, v_A=0.9) are 17.0 and 22.4 J/m^2 for the laminates sintered at 1450 and 1550ºC, respectively. In both cases, the actual work of fracture values of the laminates were higher than the linear combination, revealing additional energy consuming processes during fracture which should be associated to the presence of the large grained alumina layer. In the laminate sintered at the lowest temperature, for which less differences between the calculated and determined work of fracture existed (≅39%), there was not a macroscopic effect of the coarse grained layer

(Fig. 7a) on crack propagation. In this material, the only reinforcing mechanism would be the crack diverting effect of the larger grains, as compared to those of the finer grained layers (Fig. 5b), which would lead to a slightly larger crack front and, consequently, work of fracture values. Conversely, in the laminate sintered at the highest temperature, there was a large scale effect of the coarse layer in which significant crack branching and bridging occurred (Fig. 7b). As additional evidence of the reinforcement produced by this heterogeneous layer, the work of fracture values of specimens of this material with large notches, in which the effect of the first heterogeneous layer was partially removed because it was partially traversed by the notch (Fig. 1 and Fig. 6.c), were lower than those for specimens with the shortest notches (Table 2).

5.- Conclusions

Al_2O_3-Al_2TiO_5 laminates with "in situ" developed internal alumina layers with large grains were obtained from small grained green compacts and using the effect of TiO_2 on the microstructural development of alumina. These laminates present large work of fracture values, as compared to those of monoliths of the same composition as the layers, which are determined by the size and fracture behaviour of the "in situ" developed alumina layers. Crack branching and bridging were identified as the main toughening mechanisms.

Acknowledgements

Work supported in part by the European Community's Human Potential Programme under contract HPRN-CT-2002-00203, [SICMAC], by the projects CICYT MAT2003-00836, CAM GRMAT0707-2004 and by the grant CSIC I3P-BPD2001-1 (Spain).

References

1. Chan, H. M., Layered Ceramics: Processing and Mechanical Behavior. Annu. Rev. Mater. Sci., 1997, 27, 249-282.
2. Clegg. W. J., Controlling Cracks in Ceramics. Science, 1999, 286, 1097-1099.
3. Harmer, M. P., Chan, H.M. and Miller, G. A., Unique opportunities for microstructural engineering with duplex and laminar ceramics composites. J. Am. Ceram. Soc., 1992, 75, 1715-1728.
4. Russo, C. J., Harmer, M. P., Chan, H. M. and Miller, G. A., Design of a laminated ceramic composite for improved strength and toughness. J. Am. Ceram. Soc., 1992, 75, 3396-4000.
5. Bueno, S., Moreno, R. and Baudín, C., Design and processing of Al_2O_3-Al_2TiO_5 layered structures. J. Eur. Ceram. Soc., 2005, 25, 847-856.
6. Bueno, S., Moreno, R. and Baudín, C., Colloidal Processing of Laminates in the System Alumina-Titania**.** Key Engineering Materials, 2004, 264-268, 61-64.
7. Bueno, S. and Baudín, C., Fracture Mechanisms in Laminates in the Alumina-Titania System. Key Engineering Materials, 2005, 290, 208-213.
8. Low, I. M., Synthesis and properties of in situ layered and graded aluminium titanate / alumina composites. Materials Research Bulletin, 1998, **33**, 1475-1482.
9. Morsi, K., Keshavan, H. and Bal, S., Hot pressing of graded ultrafine-grained alumina bioceramics. Materials Science and Engineering, 2004, 386, 384-389.
10. Powers, J. D. and Glaeser, A. M., Titanium effects on sintering and grain growth of alumina. In Sintering technology, ed. R. M. German, G. L. Messing, R. G. Cornwall. Marcel Dekker INC, USA, 1996, pp 33-40.

11. Chi, M., Gu, H., Wang, X. and Wang, P., Evidence of Bilevel Solubility in the Bimodal Microstructure of TiO_2-Doped Alumina. J. Am. Ceram. Soc., 2003, 86, 1953-55.

12. Bueno, S. and Baudín, C., In situ developed alumina-aluminium titanate laminates with large microstructural differences between the layers. J. Mat. Sci., In press.

13. De Portu, G., Bueno, S., Micele, L., Baudín, C. and Pezzotti, G., Piezo-spectroscopic characterization of alumina-aluminium titanate laminates. J. Eur. Ceram. Soc., In press.

14. Sakai, M., Yoshimura, J., Goto, Y. and Inagaki, M., R-Curve Behavior of Polycrystalline Graphite: Microcracking and Grain Bridging in the Wake Region. J. Am. Ceram. Soc., 1988, 71, 609-616.

15. Bueno, S., Moreno, R. and Baudín, C., Reaction sintered Al_2O_3 / Al_2TiO_5 microcrack free composites obtained by colloidal filtration. J. Eur. Ceram. Soc., 2004, 24, 2785-2791.

16. Guinea, G. V., Pastor, J. Y., Planas, J. and Elices, M., Stress intensity factor, compliance and CMOD for a general three-point-bend beam. International Journal of Fracture, 1998, 89, 103-118.

17. Baudín, C. and Moya, J.S., Influence of Titanium Dioxide on the Sintering and Microstructural Evolution of Mullite Bodies. J. Am. Ceram. Soc., 1984, 67, C134-136.

18. Mussler, B., Swain, M. and Claussen, N., Dependence of Fracture Toughness of Alumina on Grain Size and Test Technique. J. Am. Ceram. Soc., 1982, 65, 566-572.

19. Swanson, P., Fairbanks, C., Lawn, B., Mai, Y. and Hockey, B., Crack-Interface Grain Bridging as a Fracture Resistance Mechanism in Ceramics: I, Experimental Study on Alumina. J. Am. Ceram. Soc., 1987, 70, 279-289.

Figure captions

Fig. 1.- Schematic illustration of the designed five layered laminated structure showing a bend bar and the notch orientation respect to the layers. Thick alumina layers are represented with grey colour and thin alumina-10vol% aluminium titanate composite layers are represented with white colour. Dashed lines indicate the zones where the development of large grained alumina layers due to titania diffusion occurred. Two different sizes of notches are shown with a continuous and a dotted line.

Fig. 2.- Characteristic microstructures of the studied monolithic materials. Alumina grains appear with dark grey colour and aluminium titanate of an intermediate grey shade. FE-SEM micrographs of polished and thermally etched surfaces.

a) Alumina sintered at 1450ºC, A-1450.
b) Alumina+10vol.% aluminium titanate sintered at 1450ºC, A10AT-1450.
c) Alumina sintered at 1550ºC, A-1550.
d) Alumina+10vol.% aluminium titanate sintered at 1550ºC, A10AT-1550.

Fig. 3.- Characteristic microstructures of the laminated materials. FE-SEM micrographs of polished and chemically (a, b) or thermally (c, d) etched surfaces.

a) Laminate sintered at 1450ºC with the composite layer (intermediate grey) in the centre of the micrograph, two large grained alumina layers at both sides (clearest grey) and part of the fine grained alumina layers (dark grey). The profile of TiO_2 content in the alumina layers determined by WDS analysis is shown.
b) Laminate sintered at 1550ºC with the composite layer (intermediate grey) in the centre of the micrograph, two large grained alumina layers at both sides (clearest grey) and part of the fine grained alumina layers (dark grey). The profile of TiO_2 content in the alumina layers determined by WDS analysis is shown.
c) Detail of interface between a composite layer (right) and the contiguous relatively large grained alumina layer (left) in the laminated sintered at 1450ºC.
d) Detail of interface between a composite layer (right) and the contiguous relatively large grained alumina layer (left) in the laminated sintered at 1550ºC.

Fig. 4.- Characteristic load-displacement curves of notched samples of the laminates with a relationship between the notch depth and the height of the sample of 0.14 and 0.29 (Corresponding to relative ratios of 0.4 and 0.8 of the width of the external alumina layer respectively)

a) Laminates sintered at 1450ºC. Unstable test for notch of 0.4 is shown.
b) Laminates sintered at 1550ºC.

Fig. 5.- Characteristic fracture surfaces of notched samples of the laminates sintered at 1450ºC. FE-SEM micrographs.

a) Mixed trans/intergranular fracture in the fine grained alumina layer from the tip of the notch. Specimen with a relative notch depth of 0.4 of the external alumina layer.
b) Transition between the fine and large grained alumina layer with mostly intergranular fracture. Specimen with a relative notch depth of 0.8 of the external alumina layer.
c) Intergranular fracture in the large grained alumina layer showing high levels of intergranular porosity. The composite A10AT layer is showed at the top of the micrograph.

Fig. 6.- Characteristic fracture surfaces of notched samples of the laminates sintered at 1550ºC. FE-SEM.

a) Mixed trans/intergranular fracture in the fine grained alumina layer. Specimen with a relative notch depth of 0.4 of the external alumina layer.
b) Intergranular fracture in the large grained alumina layer in a specimen with relative notch depth of 0.4 of the external alumina layer. Fine alumina layer is at the bottom and the composite layer at the top.
c) Intergranular fracture in the specimen with the largest notch (0.8). Fracture started from the large grained layer and mostly intergranular porosity was revealed by the fracture.

Fig. 7.- Optical microscopy micrographs of polished lateral faces of fractured laminated samples showing characteristic crack paths. Crack growth propagation is from the bottom to the top. Dashed lines mark the composite internal layers.

a) Laminate sintered at 1450ºC. Relative notch size 0.8 of the external alumina layer
b) Laminate sintered at 1550ºC. Relative notch size 0.4 of the external alumina layer. The large alumina grains of the in situ formed large grained alumina layer act as sites for crack branching and as bridges in the wake of the propagating crack.

Tables

Table 1. Properties of the monolithic materials (G: Grain size, K_{IC}: Fracture toughness, γ_{WOF}: Work of fracture, A: Alumina, AT: Aluminium titanate). Sd.: standard deviation.

	G_A (sd), μm	**G_{AT} (sd), μm**	**K_{IC} (sd), MPa·m$^{1/2}$**	**γ_{WOF} (sd), J·m^{-2}**
A-1450	3.5 (0.3)	-	2.9 (0.2)	14.7 (1.9)
A10AT-1450	3.2 (0.4)	2.2 (0.1)	3.5 (0.1)	34.7 (1.3)
A-1550	5.5 (0.5)	-	3.0 (0.3)	20.4 (2.8)
A10AT-1550	3.9 (0.3)	2.4 (0.2)	3.3 (0.1)	40.6 (1.2)

Table 2. Properties of the laminates (K_{IC}: Fracture toughness, γ_{WOF}: Work of fracture) 0.4 and 0.8 refers to the notch depth relative to the width of the first alumina layer (a/W_A). Sd.: standard deviation.

	K_{IC} (sd), MPa·m$^{1/2}$		**γ_{WOF} (sd), J·m^{-2}**	
	0.4	***0.8***	***0.4***	***0.8***
1450	3.1 (0.1)*	3.1 (0.2)	-*	23.7 (1.1)
1550	3.5 (0.2)	2.9 (0.1)	47.6 (1.2)	32.5 (1.3)

* Unstable tests

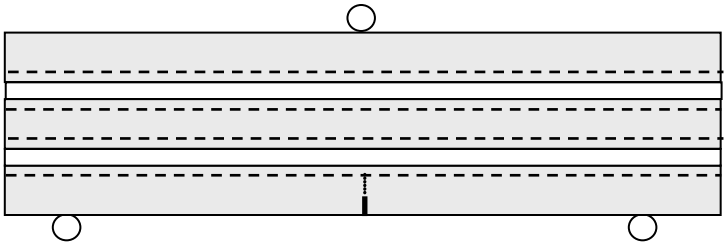

Fig. 1.- Schematic illustration of the designed five layered laminated structure showing a bend bar and the notch orientation respect to the layers. Thick alumina layers are represented with grey colour and thin alumina-10vol% aluminium titanate composite layers are represented with white colour. Dashed lines indicate the zones where the development of large grained alumina layers due to titania diffusion occurred. Two different sizes of notches are shown with a continuous and a dotted line.

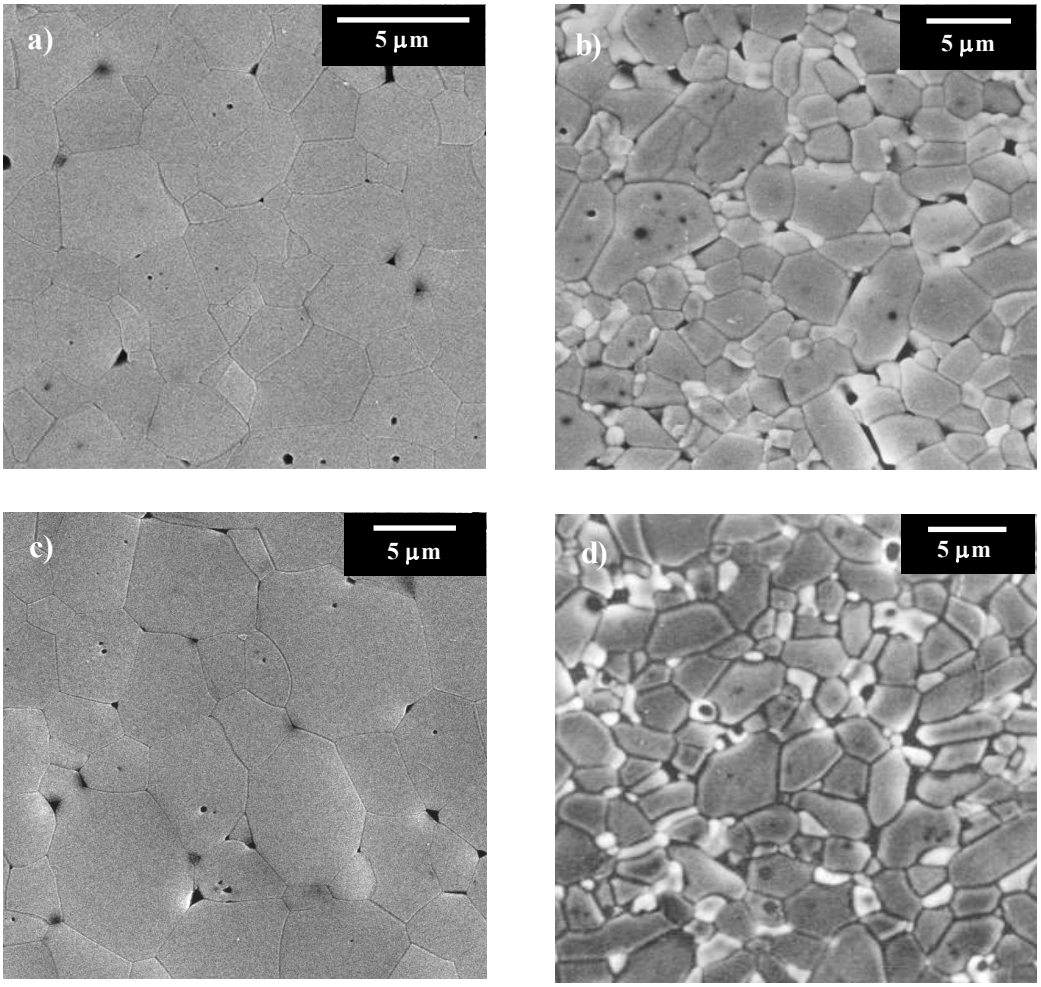
a)
5 µm
b)
5 µm
c)
5 µm
d)
5 µm

Fig. 2.- Characteristic microstructures of the studied monolithic materials. Alumina grains appear with dark grey colour and aluminium titanate of an intermediate grey shade. FE-SEM micrographs of polished and thermally etched surfaces.

a) Alumina sintered at 1450ºC, A-1450.
b) Alumina+10vol.% aluminium titanate sintered at 1450ºC, A10AT-1450.
c) Alumina sintered at 1550ºC, A-1550.
d) Alumina+10vol.% aluminium titanate sintered at 1550ºC, A10AT-1550.

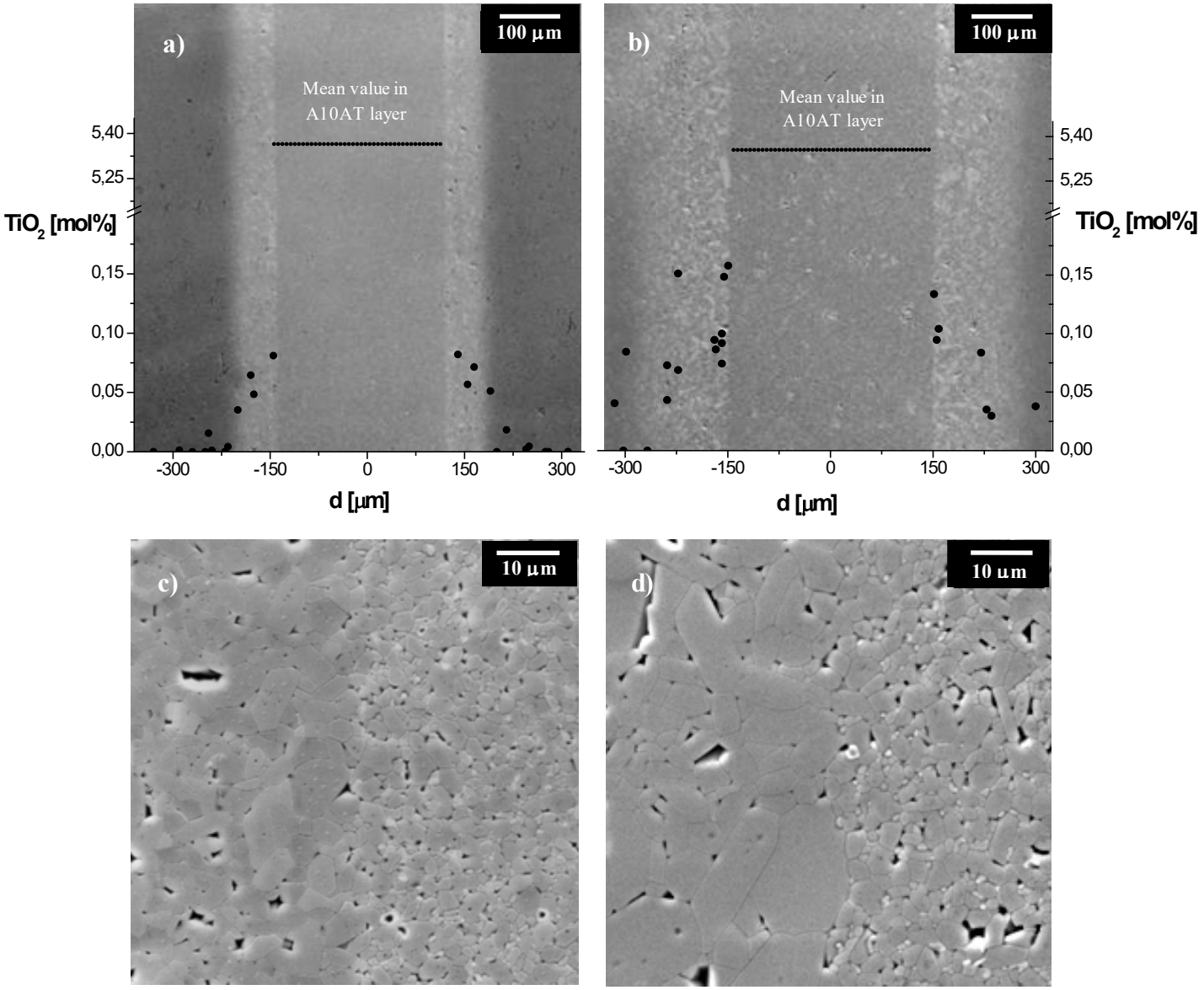

Fig. 3.- Characteristic microstructures of the laminated materials. FE-SEM micrographs of polished and chemically (a, b) or thermally (c, d) etched surfaces.

e) Laminate sintered at 1450ºC with the composite layer (intermediate grey) in the centre of the micrograph, two large grained alumina layers at both sides (clearest grey) and part of the fine grained alumina layers (dark grey). The profile of TiO_2 content in the alumina layers determined by WDS analysis is shown.

f) Laminate sintered at 1550ºC with the composite layer (intermediate grey) in the centre of the micrograph, two large grained alumina layers at both sides (clearest grey) and part of the fine grained alumina layers (dark grey). The profile of TiO_2 content in the alumina layers determined by WDS analysis is shown.

g) Detail of interface between a composite layer (right) and the contiguous relatively large grained alumina layer (left) in the laminated sintered at 1450ºC.

h) Detail of interface between a composite layer (right) and the contiguous relatively large grained alumina layer (left) in the laminated sintered at 1550ºC.

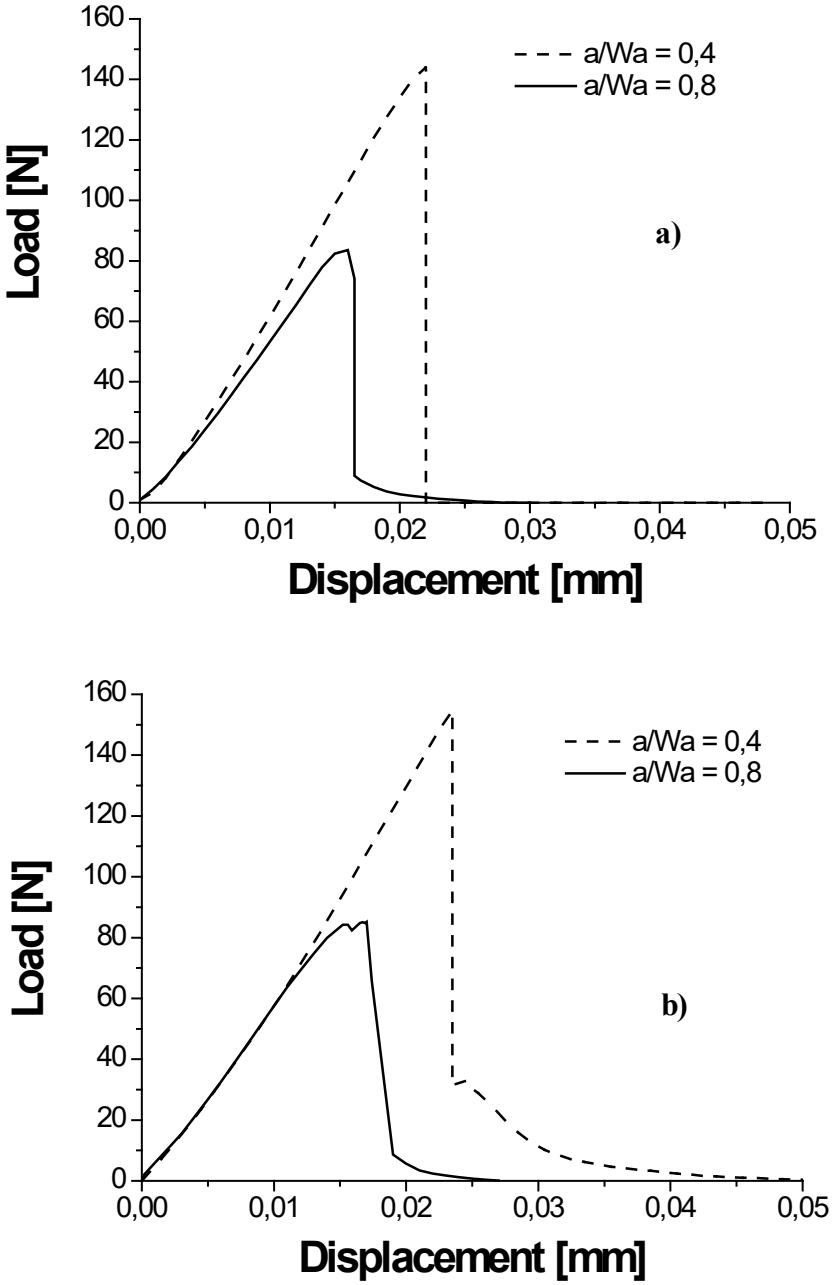

Fig. 4.- Characteristic load-displacement curves of notched samples of the laminates with a relationship between the notch depth and the height of the sample of 0.14 and 0.29 (Corresponding to relative ratios of 0.4 and 0.8 of the width of the external alumina layer respectively)

c) Laminates sintered at 1450ºC. Unstable test for notch of 0.4 is shown.

d) Laminates sintered at 1550ºC.

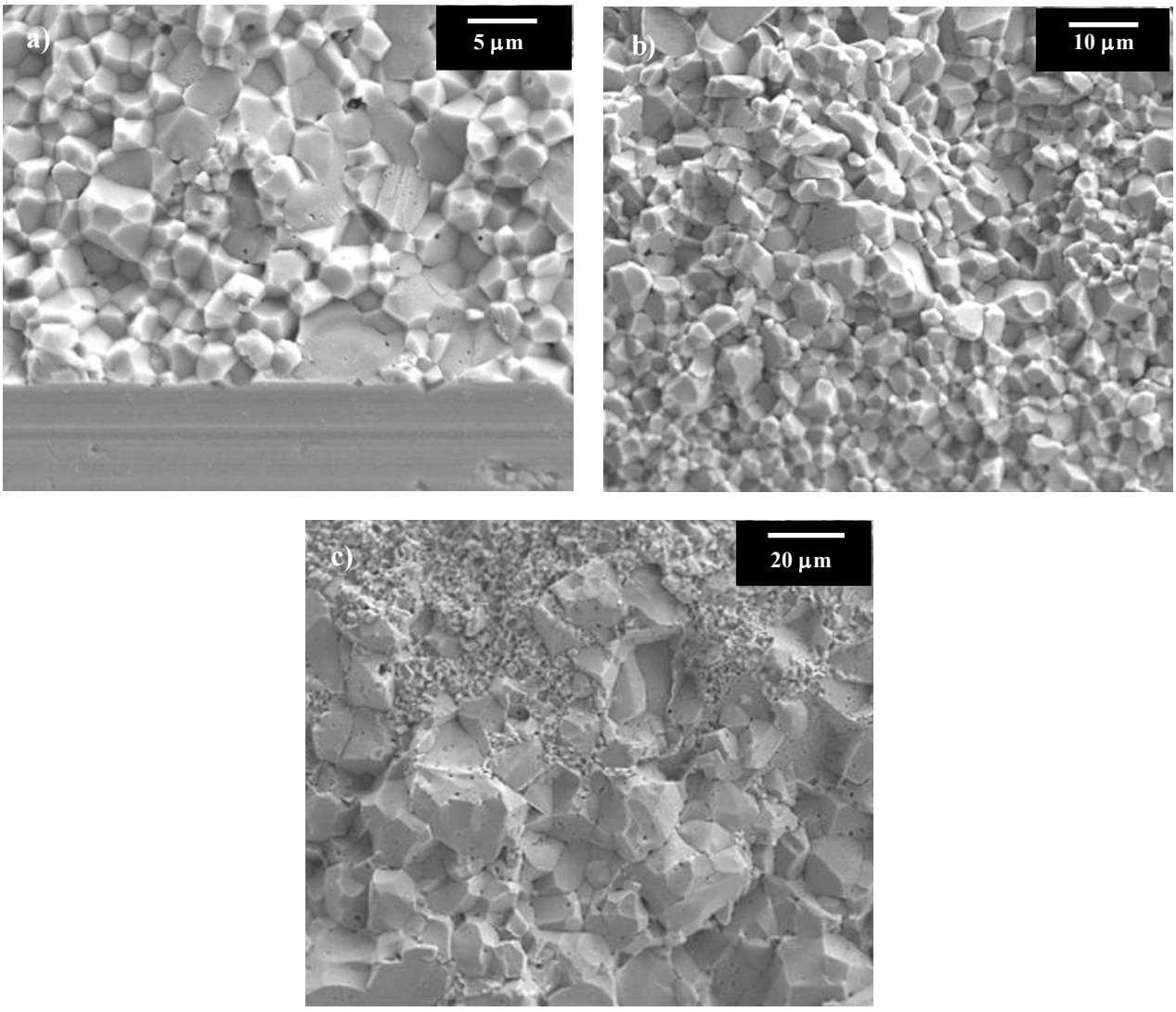

Fig. 5.- Characteristic fracture surfaces of notched samples of the laminates sintered at 1450ºC. FE-SEM micrographs.

d) Mixed trans/intergranular fracture in the fine grained alumina layer from the tip of the notch. Specimen with a relative notch depth of 0.4 of the external alumina layer.
e) Transition between the fine and large grained alumina layer with mostly intergranular fracture. Specimen with a relative notch depth of 0.8 of the external alumina layer.
f) Intergranular fracture in the large grained alumina layer showing high levels of intergranular porosity. The composite A10AT layer is showed at the top of the micrograph.

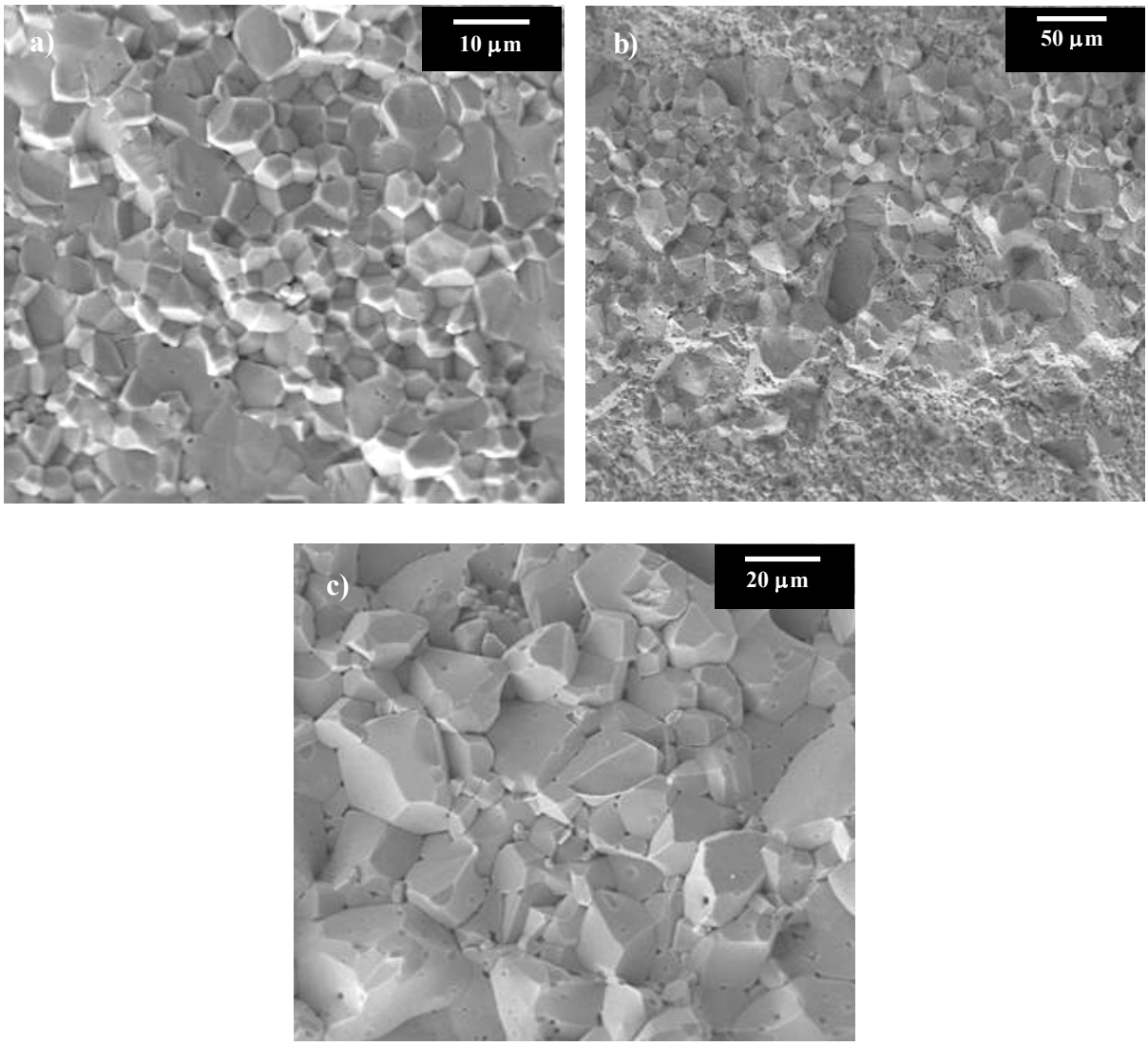

Fig. 6.- Characteristic fracture surfaces of notched samples of the laminates sintered at 1550ºC. FE-SEM.

d) Mixed trans/intergranular fracture in the fine grained alumina layer. Specimen with a relative notch depth of 0.4 of the external alumina layer.
e) Intergranular fracture in the large grained alumina layer in a specimen with relative notch depth of 0.4 of the external alumina layer. Fine alumina layer is at the bottom and the composite layer at the top.
f) Intergranular fracture in the specimen with the largest notch (0.8). Fracture started from the large grained layer and mostly intergranular porosity was revealed by the fracture.

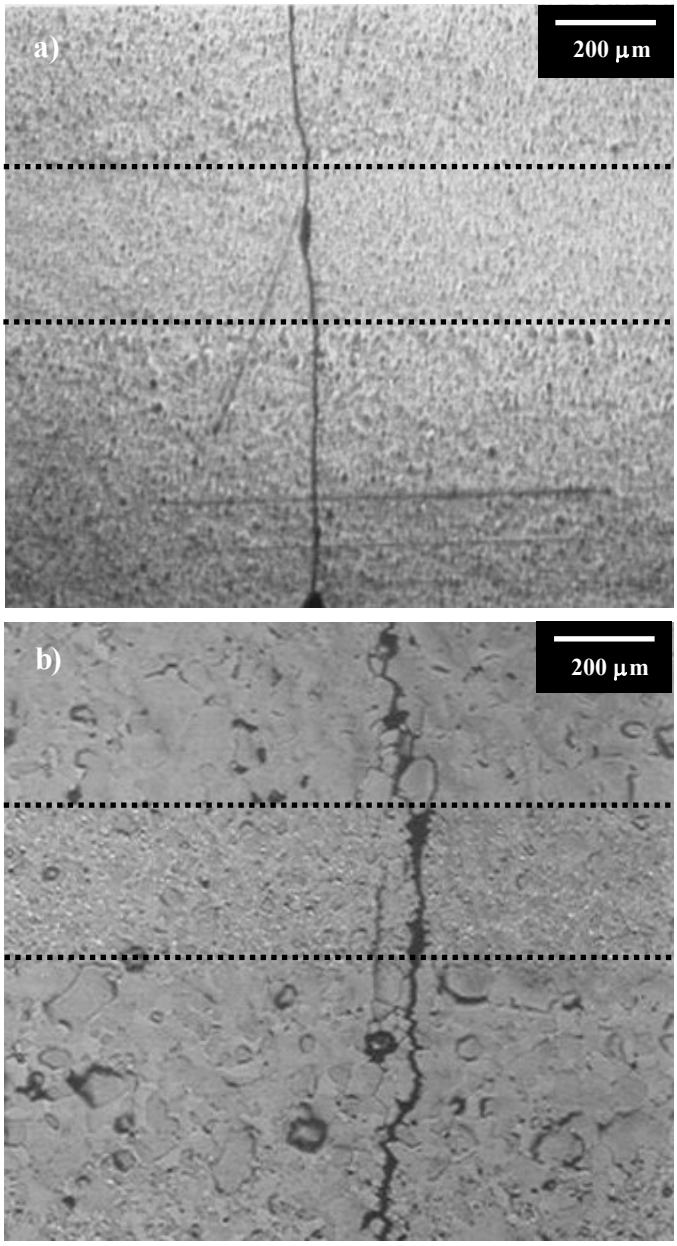

Fig. 7.- Optical microscopy micrographs of polished lateral faces of fractured laminated samples showing characteristic crack paths. Crack growth propagation is from the bottom to the top. Dashed lines mark the composite internal layers.

c) Laminate sintered at 1450ºC. Relative notch size 0.8 of the external alumina layer
d) Laminate sintered at 1550ºC. Relative notch size 0.4 of the external alumina layer. The large alumina grains of the in situ formed large grained alumina layer act as sites for crack branching and as bridges in the wake of the propagating crack.